Mon. Not. R. Astron. Soc. **341,** 863–869 (2003)

Variability of the accretion stream in the eclipsing polar EP Dra

C. M. Bridge,[1⋆] Mark Cropper,[1] Gavin Ramsay,[1] J. H. J. de Bruijne,[2] A. P. Reynolds[2] and M. A. C. Perryman[2]

[1]*Mullard Space Science Laboratory, University College London, Holmbury St. Mary, Dorking, Surrey RH5 6NT*
[2]*Research and Scientific Support Department of ESA, ESTEC, Postbus 299, 2200 AG Noordwijk, the Netherlands*

Accepted 2003 January 24. Received 2003 January 14; in original form 2002 September 6

ABSTRACT

We present the first high time resolution light curves for six eclipses of the magnetic cataclysmic variable EP Dra, taken using the superconducting tunnel junction imager S-Cam2. The system shows a varying eclipse profile between consecutive eclipses over the two nights of observation. We attribute the variable stream eclipse after accretion region ingress to a variation in the amount and location of bright material in the accretion stream. This material creates an accretion curtain as it is threaded by many field lines along the accretion stream trajectory. We identify this as the cause of absorption evident in the light curves when the system is in a high accretion state. We do not see direct evidence in the light curves for an accretion spot on the white dwarf; however, the variation of the stream brightness with the brightness of the rapid decline in flux at eclipse ingress indicates the presence of some form of accretion region. This accretion region is most likely located at high colatitude on the white dwarf surface, forming an arc shape at the foot points of the many field lines channelling the accretion curtain.

Key words: accretion, accretion discs – binaries: eclipsing – stars: individual: EP Dra – stars: magnetic fields – novae, cataclysmic variables.

1 INTRODUCTION

Polars are a subclass of magnetic cataclysmic variables. They are binary systems containing a strongly magnetic, accreting white dwarf primary (10–200 MG) and a late main-sequence secondary. The magnetic field of the primary controls the flow of material lost from the secondary and prevents the formation of an accretion disc. The material is instead confined by the magnetic field and channelled to accrete directly on to the primary through a stand-off shock; see Cropper (1990) for a review of polars.

The eclipsing nature of a small subset of these systems allows the isolation of the emission from different regions as various parts are eclipsed and revealed by the secondary. In particular, these systems are well suited to the study of the brightness distribution of the accretion stream itself, as the emission from this part of the system can be isolated once the accretion region (or regions) has been eclipsed.

In this paper we present the first high time resolution observations of the eclipses in the polar EP Dra using a detector with intrinsic time and energy resolution. The system has an orbital period of 104.6 min, and was identified as the optical counterpart to a hard X-ray source in the *HEAO-1* survey by Remillard et al. (1991). The system is faint, with an average faint phase brightness of $V \simeq 18$ in 1992 and 1995 and a maximum brightness of $V \simeq 17$ (Schwope & Mengel 1997, hereafter SM97), with evidence for accretion at one region only on the white dwarf primary (Remillard et al. 1991).

Our observations were taken with the second prototype of a new generation of optical detector (S-Cam2) which uses superconducting tunnel junctions (STJs) to record the time of arrival, location on the array and, uniquely, the energy of incident photons. For details of the instrumentation, see for example Rando et al. (2000). Previous observations of close binary systems made using S-Cam2 include UZ For (Perryman et al. 2001), HU Aqr (Bridge et al. 2002) and IY UMa (Steeghs et al. 2003).

2 OBSERVATIONS AND REDUCTIONS

The observations were made at the William Herschel Telescope (WHT), La Palma, on the nights of 2000 October 2/3 and 3/4. The S-Cam2 instrument was located at the Nasmyth focus and a total of six eclipses of EP Dra were obtained. Table 1 gives the cycle number (relative to the ephemeris of SM97), date, start time and length for each observation, as well as the time of mid-eclipse (defined as orbital phase $\phi = 0.0$), mid-ingress and mid-egress of the steep components of the eclipse (all times are in TDB – barycentric dynamical time – which includes light travel time correction to the solar system barycentre). Two of the observations (cycles 62 and 64) have data gaps caused by the instrument exceeding the data acquisition limits.

The useful observational wavelength range of S-Cam2 is 340–680 nm (Perryman et al. 2001). We split this wavelength range into

⋆E-mail: cb2@mssl.ucl.ac.uk

Table 1. Summary of observations of EP Dra for the nights of 2000 October 2/3 and 3/4. Cycle numbers are with respect to the ephemeris of SM97.

Cycle number (56900+)	Date	Start time (TDB) (2450000.0+)	Observation length (s)	Time of mid-eclipse (TDB) (2450000.0+)	Time of mid-ingress (TDB) (2450000.0+)	Time of mid-egress (TDB) (2450000.0+)
62	2000 Oct 2	1820.36254	1496	1820.37575	1820.37382	1820.37850
63	2000 Oct 2	1820.44230	1800	1820.44840	1820.44649	1820.45128
64	2000 Oct 3	1820.50681	2523	1820.52106	1820.51913	1820.52387
76	2000 Oct 3	1821.38171	2400	1821.39294	1821.39097	1821.39572
77	2000 Oct 3	1821.45653	2111	1821.46559	1821.46368	1821.46835
78	2000 Oct 4	1821.53007	1393	1821.53825	1821.53631	1821.54112

four bands, which here we label: U (340–400 nm), B (390–490 nm), V (500–600 nm) and R_C (590–680 nm). These correspond very broadly to those of the Johnson–Cousins $UBVR_C$ system (Bessell 1990, and references therein). The light curves were background subtracted using a mean value from off-source pixels taken from the mid-eclipse phases. See Perryman et al. (2001) for a detailed discussion of the data reduction process.

The 'white' light curves are shown in Fig. 1 and $UBVR_C$-bands in Fig. 2. Each figure shows the three consecutive eclipses for each of the two nights of the observations. The right-hand panel of Fig. 1 shows the eclipse of the white dwarf, accretion region and accretion stream on an expanded scale, making the rapid changes at ingress and egress more clear. The U and R_C light curves are binned in 4-s intervals, and the B and V light curves in 1-s intervals. The light curves have been calibrated in energy units using observations of the standard star BD+28 4211, which were taken on the first night. A standard star was not observed on the second night so cycles 76–78 are only approximately calibrated. The maximum brightness is $V \approx 17$ at $\phi = 1.2$, consistent with the maximum measured by SM97.

The seeing for the first night was ∼1.5 arcsec, and for the second night ∼1 arcsec. Some of the variability in the eclipses of the first night may be in part due to the occasionally poorer seeing, causing the point spread function to spill over the edges of the 6 × 6 array. A number of sharp dip features (e.g. at $\phi \sim 0.96$ in cycle 62) can be attributed to this.

3 LIGHT-CURVE FEATURES

3.1 White dwarf and accretion region eclipse

The most prominent feature of the light curves is the eclipse of the white dwarf and accretion stream by the secondary between $\phi = 0.972$ and 1.04. The duration of the eclipse (measured between the

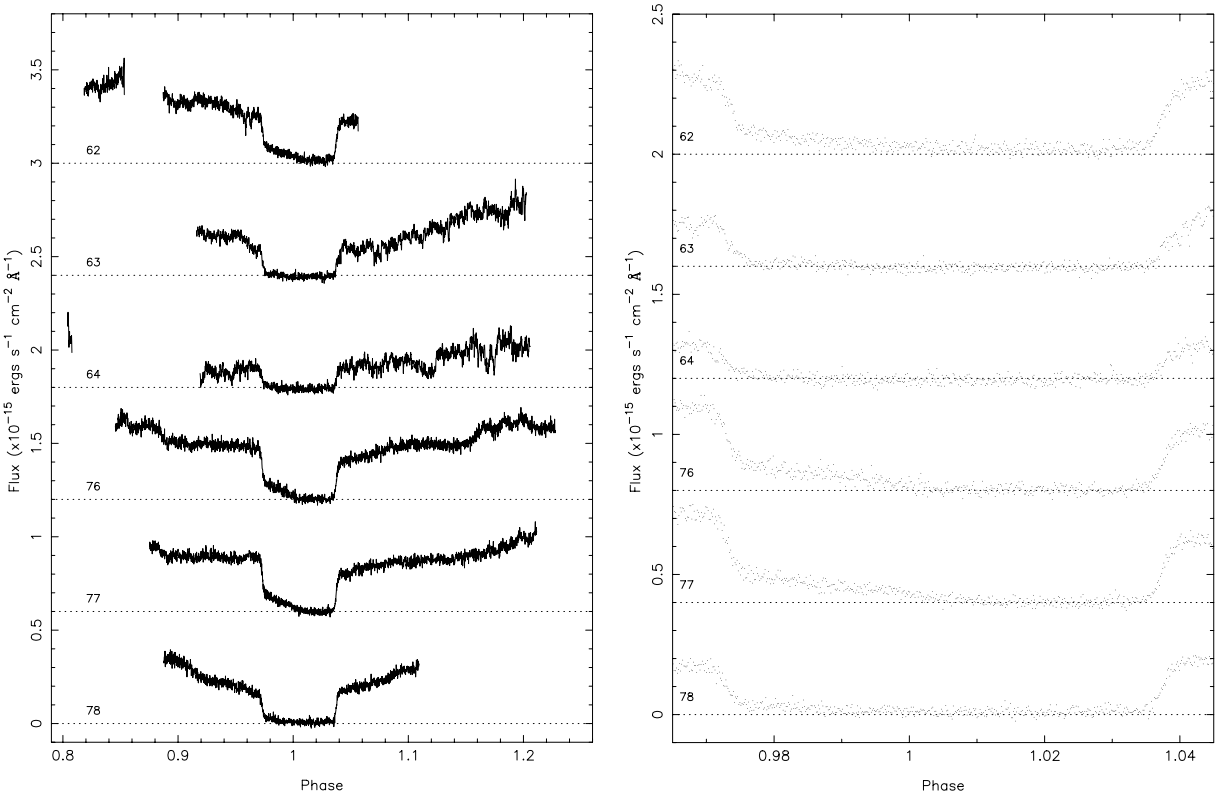

Figure 1. White light curves for EP Dra in 1-s time bins. Each cycle is offset vertically by 0.6×10^{-15} erg s^{-1} cm^{-2} Å^{-1}, and phased according to the ephemeris of SM97. The right-hand panel shows the eclipse of the accretion region and stream in more detail, highlighting the variability between consecutive eclipses. Each cycle is offset vertically by 0.4×10^{-15} erg s^{-1} cm^{-2} Å^{-1}.

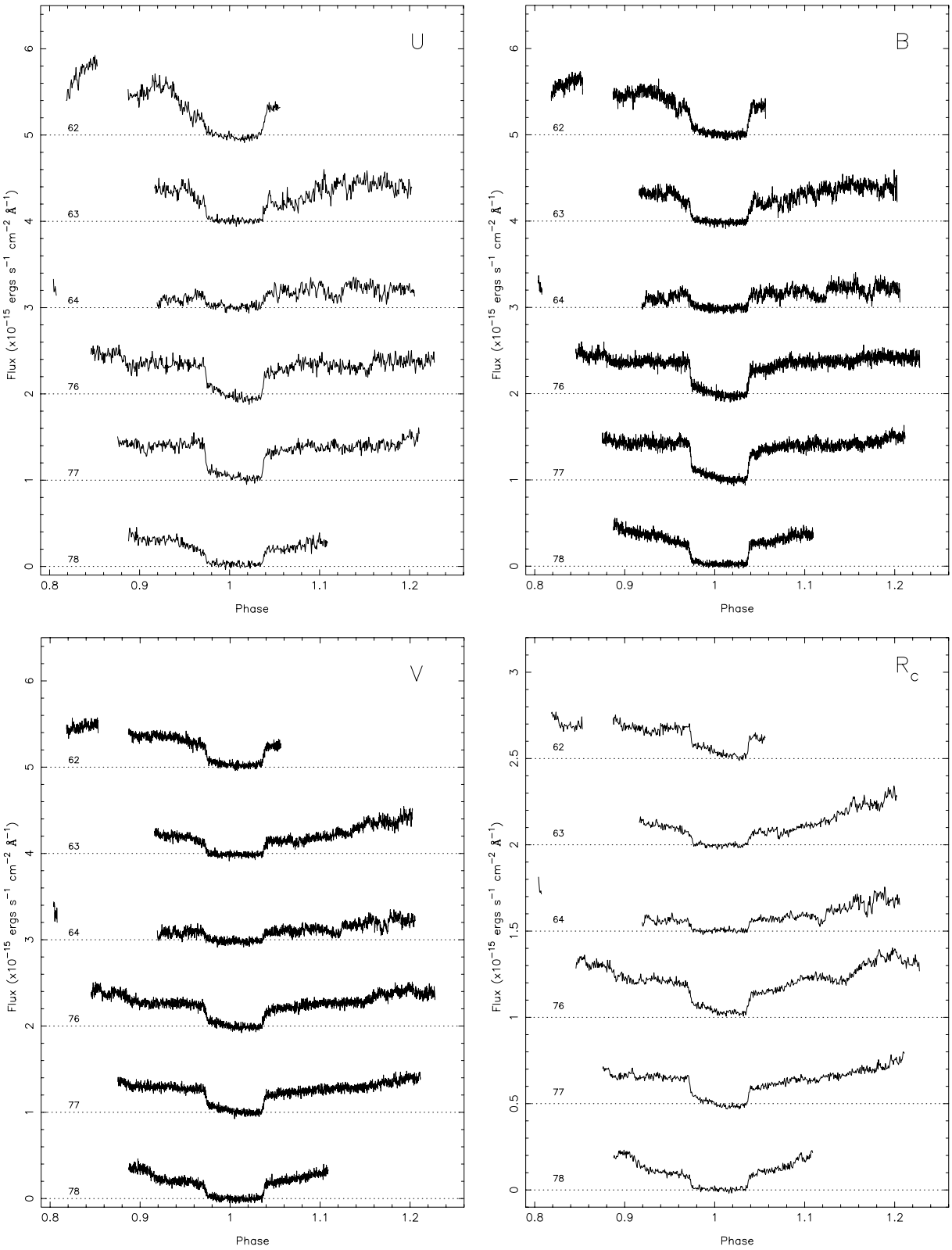

Figure 2. *UBVR*$_C$ colour light curves for the six cycles, phased with respect to the ephemeris of SM97. The *U*-band and R_C-band light curves are binned in 4-s time bins due to low count rates. The *B*-band and *V*-band are in 1-s time bins. Note the vertical scale for the R_C-band is smaller due to the lower flux in this band.

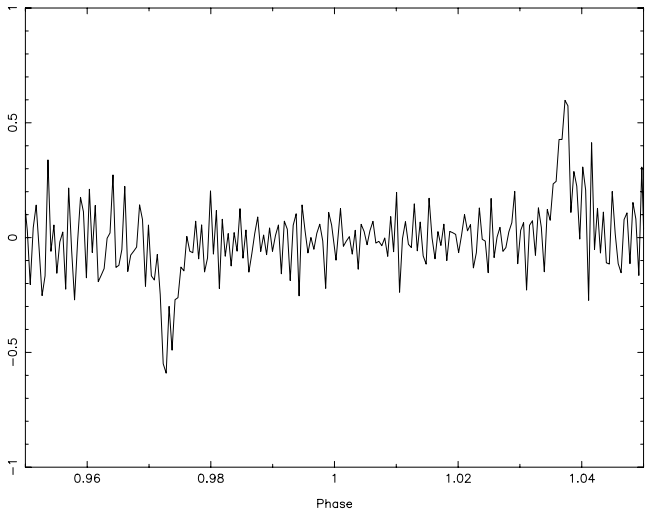

Figure 3. The mean of the six 3-s differential white light curves.

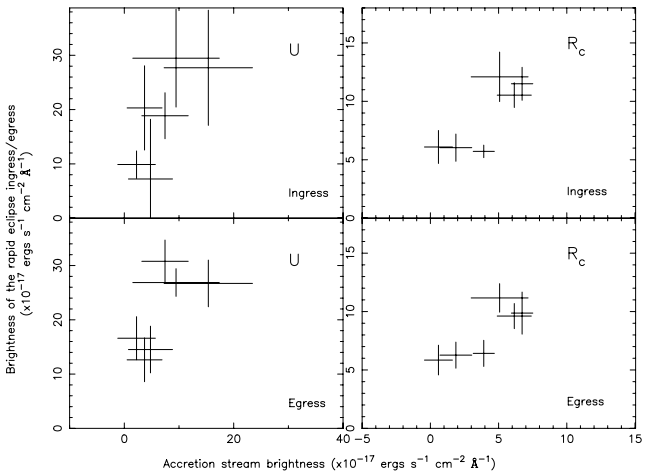

Figure 4. The amplitude of the rapid brightness change at ingress and egress against the brightness of the accretion stream. This is shown for both the U-band and R_C-band light curves. The stream brightness is measured immediately after the steep eclipse ingress at $\phi = 0.975$.

middle of the steep eclipse components) is the same for all cycles, 6.8 min, equivalent to $\Delta\phi = 0.0646$.

The eclipse of the white dwarf photosphere and the accretion region is very rapid. To characterize the rapid eclipse we binned the six white light curves into 3-s time bins, then for each time bin we subtracted the brightness of the previous time bin. Fig. 3 shows the mean of these six differential light curves. The width of the complete ingress and egress of the white dwarf and accretion region is 36 s, which is comparable to the expected ingress duration for the white dwarf of 37 s (assuming a primary mass $M_1 = 0.43\,\mathrm{M}_\odot$ and mass ratio $q = 0.31$; SM97). The amplitude of the brightness change at ingress is greatest at bluer wavelengths, which is as expected for a hot accretion region and white dwarf.

HU Aqr (Bridge et al. 2002) and UZ For (Perryman et al. 2001) show a rapid drop in flux at eclipse ingress lasting a few seconds, which is taken as evidence of a bright, compact accretion region. In contrast, we see no evidence for such a rapid drop in EP Dra. However, there is some asymmetry in Fig. 3 which implies the presence of an accretion region in some form.

Following the rapid 36-s decline in brightness seen at ingress, the stream is the major contributor to the observed brightness, with only a small amount of emission from the secondary in the red. The presence of an accretion region is also evident from our observation that the amplitude of the rapid ingress varies with the brightness of the accretion stream, and this is illustrated in Fig. 4. If there was no contribution from an accretion region, then we would expect no correlation. We therefore identify the rapid decline in flux with the eclipse of both the white dwarf and an accretion region, despite the accretion region not being directly evident in the eclipse. By comparison with HU Aqr and UZ For, the absence of a compact accretion region is surprising.

3.2 Stream eclipse

In our light curves, the stream eclipse ingress, from $\phi \simeq 0.975$ onwards, takes two forms: a long ingress from a relatively bright stream (cycles 62, 76 and 77) and a short ingress from a faint stream (cycles 63, 64 and 78). Fig. 5 shows the eclipse profile of all six cycles, and the two forms of stream eclipse are clear. We also see that there is a decline in flux preceding the ingress of the white

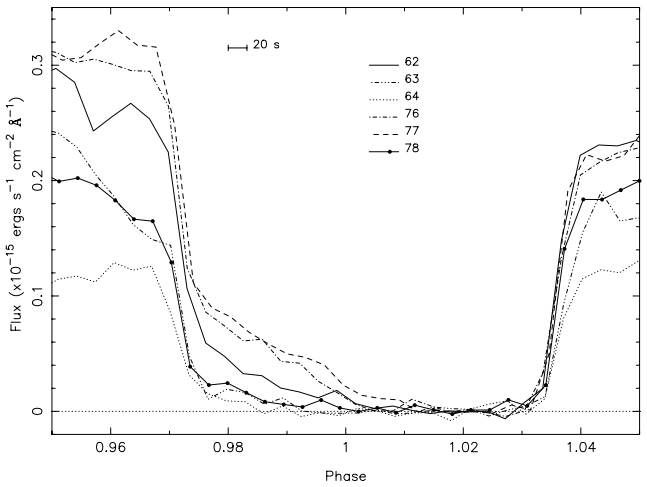

Figure 5. The six white light curves centred on the eclipse by the secondary. They have been binned into 20-s time bins, which removes any features related to the eclipse of the white dwarf and the accretion region, and the secondary contribution has been subtracted.

dwarf and accretion region in cycles 63 and 78 where the stream is relatively faint.

3.3 Out of eclipse

The prominent feature before and after the eclipse is the decline in brightness at phase $\phi = 0.874$ in cycle 76 and subsequent rise at $\phi = 1.16$. This is seen in all bands in Fig. 2. The duration of the decline is $\sim$100 s, ending at $\phi = 0.89$. The reduced phase coverage in cycle 77 means that we cannot be certain that the feature at $\phi = 0.88$ is the same feature as that in the preceding cycle. However, the similarity in the shape of the light curve compared to that of cycle 76 and the location of the feature means that we proceed assuming they are the same. We refer to this pre-eclipse decline and post-eclipse rise as the 'trough'.

There is a bright stream in cycle 76; however, in cycle 78 the stream is fainter and we identify the trough as starting at the later

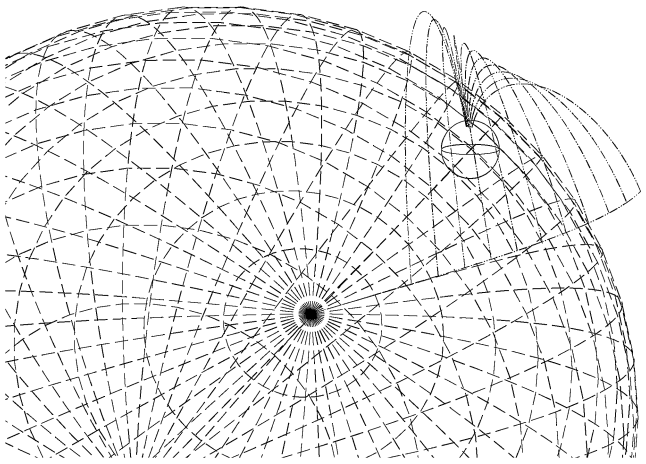

Figure 6. Plot of the geometry of EP Dra consistent with a variable brightness stream for $\phi = 0.98$. The magnetic field lines are still visible, causing a long stream ingress in the light curves for bright stream material confined to these field lines. The magnetic pole is located at $\beta = 18.0^\circ$ and $\zeta = -17.0^\circ$ (assuming the values for the accretion region in Remillard et al. (1991) are the same as the magnetic pole).

phase of $\phi = 0.90$. We also infer that the rise at $\phi = 1.08$ in cycle 78 is the counterpart of that at $\phi = 1.16$ in cycle 76.

Following the start of the trough, cycles 76 and 77 show a relatively flat light curve prior to the eclipse of the white dwarf. In cycles 62, 63 and 78, after $\phi = 0.95$, there is a decline in flux prior to the eclipse ingress.

After the rapid egress of the white dwarf photosphere and accretion region at $\phi = 1.04$, there is no obvious stream egress in cycles 63 and 64, corresponding to a lack of a stream brightness at ingress. In cycles 76, 77 and 78, the accretion stream egress is seen as a gradual increase in flux, followed by a relatively flat light curve in cycles 76 and 77.

4 DISCUSSION

4.1 Accretion region location

In determining the location of material confined to magnetic field lines, the values chosen for R_μ (the distance from the white dwarf at which material is threaded by the field lines), and the colatitude (angle measured from the spin axis of the white dwarf) and longitude of the accretion region are important. Two different estimates for the location of this region are proposed by Remillard et al. (1991) and SM97. Based primarily on their circular polarimetry data, Remillard et al. (1991) concluded that there was only one accretion region, at a colatitude of $\sim 18^\circ$ and longitude $\sim -17^\circ$. On the other hand, SM97, modelling the bright cyclotron peaks in optical observations, found a colatitude of $\sim$60–70°.

As we are unable to say with certainty what the true location of the accretion region is, we consider both possibilities of high and low latitude accretion in the following discussion. To proceed we use the mass ratio ($q = 0.31$; SM97) to create a model Roche lobe and white dwarf with a magnetic pole at a given colatitude, β, and longitude, ζ. Dipole field lines are then constructed passing through a given R_μ. By varying R_μ for a given magnetic pole location, field lines can be created that eclipse a given part of the polar system at a phase given by features observed in the light curves. Although Remillard et al. (1991) and SM97 quote the location of the accretion region, we use these values for the location of the magnetic pole, noting that this will cause accretion at a region offset from these values for a given R_μ.

4.2 Stream variations

The observed stream variations (Figs 1 and 5) are essentially caused by a change in the visibility of material confined to the magnetic field lines of the white dwarf. This could be caused by an asynchronism in the white dwarf spin and orbital periods, causing a changing magnetic field to be presented to the incoming accretion stream. However, we consider this unlikely due to a lack of change in the relative position of the bright phase and eclipse between the observations of Remillard et al. (1991) and SM97.

Alternatively, there is either a change in the amount of bright material on visible field lines or material is located on different field lines. These can be caused by a change in R_μ, from a variation in the mass transfer rate and an inhomogeneity in the flow. It is not possible from our data to isolate either possibility as the cause, and it is probable that both contribute to the observed stream variability. Variations in the accretion stream eclipse profile have been observed in many eclipsing polars, for example in HU Aqr (Glenn et al. 1994; Harrop-Allin et al. 1999; Bridge et al. 2002) and V895 Cen (Salvi et al. 2002).

We can estimate R_μ from the phase at which visible magnetic field lines are completely eclipsed in our geometric model, Fig. 6. We find that a longer stream ingress requires a smaller R_μ for a high colatitude accretion region (SM97), compared with that from a low colatitude (Remillard et al. 1991).

4.3 Trough feature

We consider two mechanisms that could explain the trough: absorption or emission. Absorption would occur from material lost by the secondary, with the initial drop in the light curves resulting from the onset of the absorption. Alternatively, the feature could be caused by the changing cyclotron emission with phase.

4.3.1 Emission

SM97 observed a sharp rise to and decline from the bright phase (which is indicative of the cyclotron beaming effect) in their V-band light curves of EP Dra. The phase range of our light curves is much less than that of SM97 so we do not observe the same behaviour either side of the eclipse; however, the trend of our light curves is consistent with such a rise to and fall from maximum. Fig. 7 shows our V-band light curves with the SM97 figure 1 V-band data from 1995. The SM97 data have been scaled vertically to show the coincidence of the features.

The wavelength at which the cyclotron emission peaks is dependent upon the magnetic field strength of the white dwarf, with increasing field strength shifting the peak to shorter wavelengths. For EP Dra, the field is $\sim$16 MG (SM97) so we would expect the orbital variability to be greatest towards redder wavelengths. We therefore expect to see a significant change in the shape of the light curves in the different colour bands, and hence a prominent feature in the colour ratios. As a signature of the cyclotron emission, we would expect a sharp peak in the R_C-band followed by a gradual decline, and conversely in the U-band a more gradual rise in flux to a maximum at $\phi \approx 0.97$, at which point the accretion region is eclipsed, as for example in WW Hor (Bailey et al. 1988, their figure 1).

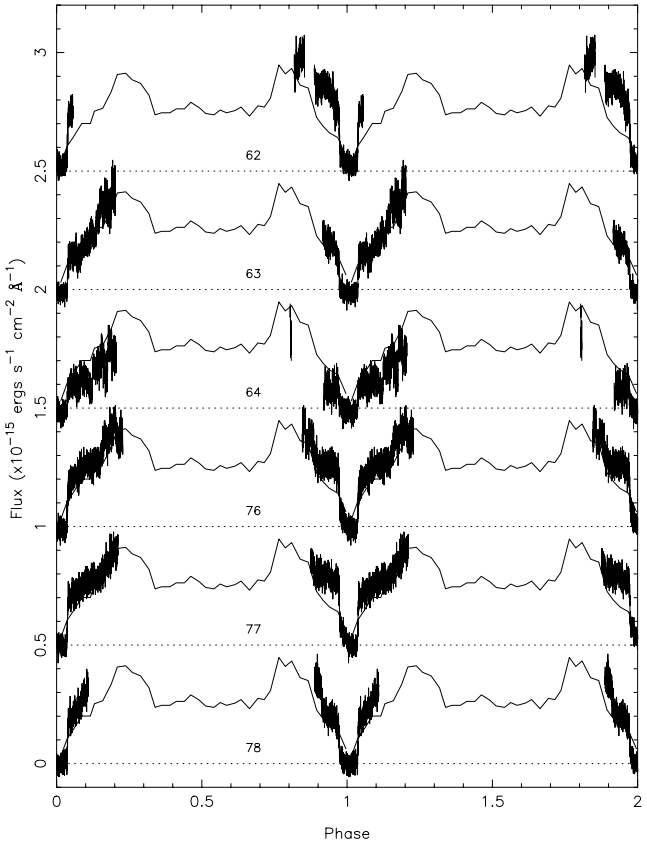

Figure 7. The *V*-band light curves of EP Dra plotted on the same phase range as those of SM97 (their figure 1). Overplotted as a solid line is their 1995 *V*-band observation for comparison.

Thus, while there is evidently some cyclotron beaming, the absence of any significant features in the light curves or consistent variations in the colour ratios implies that cyclotron beaming is only partially responsible for the observed light-curve shape, and cannot explain the flat light-curve pre-eclipse and post-eclipse.

4.3.2 Absorption

A second possible cause of the trough is absorption by obscuring material lost from the secondary in an accretion flow. This would be supported by the correlation between the presence of this feature and the brightness of the stream (Section 3.3), and also changes in R_μ caused by differing amounts of material in the stream (Section 4.2).

We see a reddening in the U/R_C colour ratios during the decline in flux in cycle 76 between $\phi \approx 0.88$ and 0.89. This effect is more pronounced in cycle 78 where there is a significant dip towards the red and a rise to the blue again during the extended decline between $\phi \approx 0.89$ and 0.925. In the *U*-band and *B*-band of cycle 62, we see a rise in flux and a corresponding decrease in the R_C-band at phases corresponding to the end of the extended decline in cycle 76. The most likely cause is the onset of absorption by material in the accretion stream. The increased absorption at shorter wavelengths is contrary to the expected free–free absorption in the accretion stream (King & Williams 1985), which predicts increasing absorption at longer wavelengths (Watson et al. 1995).

The observed variation of the light curves with the colour ratios suggests that the absorption process is likely to be bound–free absorption of the Balmer continuum. This is predominantly in the *U*-band, and the variations in the colour ratios and light curves are explained by variations in the amount and density of material confined by the magnetic field lines of the white dwarf.

4.4 The accretion flow

The phase of the onset of the trough is later than that of the pre-eclipse dip seen in the light curves of HU Aqr (Harrop-Allin et al. 1999; Bridge et al. 2002), which was identified as the eclipse of the accretion region by the strongly collimated accretion stream. This phase is determined by the geometry of the field lines carrying the accreting material, so a difference between systems is not unexpected. While the onset of the trough feature is consistent with an eclipse caused by the accretion stream, an extended accretion curtain would cause absorption over an extended phase range (previous section), and produce the observed flat light curves during the trough (Figs 1 and 2). The extent of this accretion curtain can be estimated using the eclipse light-curve features and the geometric model introduced earlier.

A value of R_μ can be estimated by varying the parameter until the field lines begin to eclipse the accretion region, at the phase set by the start of the trough in the light curve. For those cycles with brighter streams and accretion regions, where the onset of the trough is earlier, we find values of $R_\mu \sim 0.14a$ (for $\beta = 65^\circ$) and $0.19a$ (for $\beta = 18^\circ$). For those cycles where the onset of the trough is later at $\phi = 0.90$, we find $R_\mu \sim 0.16a$ (for $\beta = 65^\circ$) and $0.22a$ (for $\beta = 18^\circ$). The outer edge of the curtain, where material threads closest to the secondary, can be estimated from the end of the egress of bright stream material around $\phi = 1.1$, and is independent of β. This assumes that there is no significant continuum emission from the ballistic section of the accretion stream, where material is expected to be faint and cooling as it falls. For those cycles where the bright stream egress is clearly seen, we find a value of $\sim 0.42a$. For those cycles with fainter streams, the egress of the stream is not seen. We therefore infer that brighter streams result in a wider accretion curtain, with more material in the accretion stream penetrating further into the magnetosphere.

For faint stream cycles, a decline in flux is seen immediately before the eclipse of the accretion region (see Section 3.2). This could be due to the eclipse of stream material which is threading early in the trajectory, and which should emit through magnetic heating. Alternatively, the decline could be caused by absorption by material along the line of sight to the white dwarf and accretion region (see Section 4.3).

The trough is absent in the observations of Remillard et al. (1991) and SM97. The stream also appears to be fainter in both previous observations, although this may be due to the poorer sampling. The lack of a bright stream may be the cause of this absence of a trough in their light curves, if the two are linked as we suggest.

An extended accretion curtain with material being threaded at different R_μ would allow material to accrete over an extended region on the white dwarf. The foot points of the field lines form an arc shape on the white dwarf surface. Such an extended accretion region would be consistent with the optical cyclotron models of SM97, which show evidence for an accretion arc or ribbon.

5 CONCLUSIONS

We have analysed the first high signal-to-noise ratio and high time resolution data of EP Dra taken on two consecutive nights at the WHT using S-Cam2. The eclipse light curves show variability in the accretion stream and accretion region over the time-scale of the

orbital period. We see no direct evidence in the light curves for the expected rapid eclipse of a small accretion region on the white dwarf. The rapid eclipse seen in the light curves is a combination of emission from the white dwarf photosphere and the accretion region. We see evidence for the variability of the accretion region from the variation in brightness of the rapid eclipse ingress with the varying accretion stream brightness.

Variability seen in the light curves on a longer time-scale is influenced to some extent by cyclotron beaming. However, from the colour dependence, there is probably also a contribution from absorption, and this is seen as a trough in the light curves of the second night. We attribute the absorption to bound–free absorption by material in an extended accretion curtain obscuring the accretion region and white dwarf. There may also be significant absorption by material located close to the white dwarf above the accretion region.

Accreting material is threaded on to many field lines along the accretion stream trajectory, and the location in phase of the onset of the trough or absorption dip provides an estimate of the location of the edge of the accretion curtain. Variations in the brightness of the accretion stream seen after the ingress of the white dwarf and the accretion region are caused by a change in the location of bright stream material in the accretion curtain and/or a change in the extent of the curtain. From the extent of the accretion curtain we infer the presence of an extended accretion arc at the foot points of the accreting field lines, however this region is still small compared with the size of the white dwarf.

ACKNOWLEDGMENTS

We acknowledge the contributions of other members of the Research and Scientific Support Department of the European Space Agency at ESTEC involved in the optical STJ development effort, in particular S. Andersson, D. Martin, J. Page, P. Verhoeve, J. Verveer, A. Peacock and N. Rando. We acknowledge the excellent support given to the instrument's operation at the WHT by the ING staff, in particular P. Moore and C. R. Benn. We would also like to thank Pasi Hakala for valuable discussions.

REFERENCES

Bailey J., Wickramasinghe D. T., Hough J. H., Cropper M., 1988, MNRAS, 234, 19
Bessell M. S., 1990, PASP, 102, 1181
Bridge C. M. et al., 2002, MNRAS, 336, 1129
Cropper M., 1990, Space Sci. Rev., 54, 195
Glenn J., Howell S. B., Schmidt G. D., Liebert J., Grauer A. D., Wagner M., 1994, ApJ, 424, 967
Harrop-Allin M. K., Cropper M., Hakala P. J., Hellier C., Ramseyer T., 1999, MNRAS, 308, 807
King A. R., Williams G., 1985, MNRAS, 215, 1p
Perryman M. A. C., Cropper M., Ramsay G., Favata F., Peacock A., Rando N., Reynolds A. P., 2001, MNRAS, 324, 899
Rando N., Verveer J., Andersson S., Verhoeve P., Peacock A., Reynolds A., Perryman M. A. C., Favata F., 2000, RScI, 71, 4582
Remillard R. A., Stroozas B. A., Tapia S., Silber A., 1991, ApJ, 379, 715
Salvi N., Ramsay G., Cropper M., Buckley D. A. H., Stobie R. S., 2002, MNRAS, 331, 488
Schwope A. D., Mengel S., 1997, AN, 318, 25 (SM97)
Steeghs D., Perryman M. A. C., Reynolds A., de Bruijne J. H. J., Marsh T., Dhillon V. S., Peacock A., 2003, MNRAS, 339, 810
Watson M. G. et al., 1995, MNRAS, 273, 681

This paper has been typeset from a TEX/LATEX file prepared by the author.